Biochimica et Biophysica Acta 893 (1987) 524–533
Elsevier

BBA 42612

Temperature dependence of S-state transition in a thermophilic cyanobacterium, *Synechococcus vulcanus* Copeland measured by absorption changes in the ultraviolet region

H. Koike [b], B. Hanssum [a], Y. Inoue [b] and G. Renger [a]

[a] *Max-Volmer-Institut für Biophysikalische und Physikalische Chemie der Technischen Universität Berlin, Berlin (Germany) and* [b] *Solar Energy Research Group, The Institute of Physical and Chemical Research (RIKEN), Wako, Saitama (Japan)*

(Received 3 March 1987)

Key words: Photosystem II; S-state transition; Temperature dependence; Spectroscopy; Water splitting; Thermophilic cyanobacterium; Cyanobacterium; (*S. vulcanus* Copeland)

The temperature dependence of S-state transition kinetics was measured by spectroscopy in the ultraviolet region with O_2-evolving Photosystem II particles from a thermophilic cyanobacterium. By proper selection of ferricyanide concentration and the measuring wavelength, the absorption changes due to S-state transitions were explicitly measured with minimized superposition of binary absorption changes due to acceptor side reactions. The half-times of $S_1 \rightarrow S_2$, $S_2 \rightarrow S_3$ and $S_3 \rightarrow S_0$ transitions were 60, 60 and 800 μs, respectively, at 50 °C, the optimal temperature for oxygen evolution by the particles, but were slowed down to 70, 120–150 and 1300 μs at 25 °C, and 106, 300 and 5500 μs at 1 °C, respectively. In the whole range of 1–50 °C the Arrhenius plots showed no break or discontinuity for $S_1 \rightarrow S_2$ and $S_2 \rightarrow S_3$ transitions, with apparent activation energies of 9.6 and 26.8 kJ/mol, respectively. The Arrhenius plot for $S_3 \rightarrow S_0$ transition, however, was composed of two straight lines with a clear break at 16 °C, and the apparent activation energies above and below the break temperature were 15.5 and 59.4 kJ/mol, respectively. The implications of these data and especially of the break temperature for the $S_3 \rightarrow S_0$ transition were discussed.

Introduction

Thermophilic cyanobacteria are unique photosynthetic organisms which grow at high temperatures, where O_2 evolution by mesophilic plants is completely inactivated [1–3]. Optimal temperatures for O_2 evolution and electron transport of these algae are found at 50–60 °C in isolated PS II particles as well as in cells and thylakoid membranes [2–5]. These facts suggest that they have adapted themselves to higher temperatures at the sacrifice of photosynthetic efficiency at lower temperatures. For instance, photosynthetic activities of these algae largely decrease at suboptimal temperatures around 30 °C and the cells do not grow at all [2]. Thus, it is of interest to characterize their electron transport reactions at the lower side of their optimal temperatures as well as their heat stability at high temperatures.

At sub-zero temperatures, the S-state transitions in these algae become inhibited step by step

Abbreviations: Chl, chlorophyll; DCBQ, 2,6-dichlorobenzoquinone; LDAO, lauryldimethylamine *N*-oxide; PS II, Photosystem II; Z, secondary electron donor of Photosystem II; Hepes, 4-(2-hydroxyethyl)-1-piperazineethanesulfonic acid; Mes, 4-morpholineethanesulfonic acid.

Correspondence: H. Koike, Solar Energy Research Group, The Institute of Physical and Chemical Research (RIKEN), Wako, Saitama 351-01, Japan.

from a higher oxidation state to a lower one, as in higher plants [6–9]. By means of thermoluminescence measurements, we have shown that in thermophilic cyanobacterial thylakoids, the lower limiting temperatures for $S_2 \rightarrow S_3$ and $S_3 \rightarrow S_0$ transitions are shifted to higher temperatures, as compared with those in spinach, while for the $S_1 \rightarrow S_2$ transition this threshold is the same as in spinach [8]. However, we would like to emphasize that these limiting temperatures are those determined by the extent of thermoluminescence B-band which arises from charge recombination between S_2 or S_3 and Q_B^- [10,11], the finally stabilized states of PS II charge separation. Thus, in strict sense, the threshold temperatures determined by thermoluminescence measurements reflect the probability of stabilization of the separated charges among the reaction centers.

In this communication, we focused our study on a more dynamic aspect, the temperature dependence of the rate of S-state transitions, and measured the kinetics of ultraviolet absorbance changes due to S-state transitions between 1 and 50 °C, using the O_2-evolving PS II particles prepared from *Synechococcus vulcanus* Copeland as experimental sample. The results indicated that each S-state transition has a specific activation energy, and the activation energy for $S_3 \rightarrow S_0$ transition shows a specific discontinuity at 16 °C, indicative of a drastic conformational change of water oxidase at low temperatures.

Materials and Methods

Highly active O_2-evolving PS II particles were prepared from a thermophilic cyanobacterium, *S. vulcanus* Copeland, basically according to the method we described previously [5,12]. However, the density gradient centrifugation used in the previous method was replaced by a fractional centrifugation: the LDAO-solubilized thylakoids were diluted 3-fold with 25% (v/v) glycerol, 10 mM $MgCl_2$ and 20 mM Hepes-NaOH (pH 7.0), and centrifuged at 180000 × *g* for 1 h at 2 °C to remove PS I particles, and then the resulting supernatant was centrifuged at 200000 × *g* for 17–18 h at 2 °C to pellet PS II particles. The PS II particles thus obtained were suspended in the same medium and stored at −196 °C until use.

This new fractionation procedure was advantageous in the following respects: a larger amount of thylakoids (240 mg Chl instead of 20 mg Chl) could be treated as one batch in a shorter time (20 h instead of 40 h) with minimized loss in PS II activity, although P-700 contamination was slightly higher (1/350–500 instead of 1/500–1000). The PS II particles obtained by this procedure contained one Q_A/45–55 Chl *a*, as determined by spectrophotometry at 325 nm based on the extinction coefficient of Q_A reported by Van Gorkom [13], and evolved O_2 at a rate of 2800 μmol O_2/mg Chl per h with $Fe(CN)_3$ as electron acceptor at 50 °C, the optimal temperature. The maximal rate of 3500–4000 μmol O_2/mg Chl per h was observed with DCBQ as acceptor at 40 °C. Activity measurements with DCBQ at 50 °C were impossible, due to degradation of this electron acceptor [2].

The PS II particles (equivalent to 10 μM Chl *a*) were suspended in 5 mM $MgCl_2$/10 mM NaCl/20 mM Mes-NaOH (pH 6.0), and illuminated with light pulses from a frequency-doubled Nd-YAG laser (5–7 ns, $\lambda = 532$ nm) in a cuvette with an optical pathlength of 1 cm, and the light-induced absorption changes were measured in the ultraviolet region, as described in Refs. 14, and 15. The temperature of the sample was controlled by thermostatted water circulating through a water-jacketted cuvette.

Results and Discussion

Light-induced absorption changes of PS II particles in the ultraviolet region

Transient ultraviolet absorption changes in a few ms time scale induced by a flash train in dark-adapted PS II preparations are basically composed of two components: one due to redox reactions of (Q_AQ_B), the acceptor quinone system, and the other due to those of the Mn-enzyme for water oxidation [13–22]. Besides these two components, absorption changes must be taken into account that are caused by the turnover of Z, which couples the water-oxidizing enzyme system with the reaction center [14,18,21,23,24]. In order to measure the absorption changes due to redox reactions in the water oxidase system, it is necessary to find a suitable condition which eliminates

or minimizes the binary-type absorption changes arising from (Q_AQ_B) redox reactions. This has been shown possible by controlling the $Fe(CN)_3$ concentration in the reaction medium [26]. The requirements of this condition are as follows. (1) All $(Q_AQ_B)^-$ must be oxidized by $Fe(CN)_3$ in the initial dark-adapted state. (2) The $Fe(CN)_3$ concentration must be high enough to reoxidize $(Q_AQ_B)^-$ generated by a preceding flash in the interval (1 s) of the flash train, but simultaneously it should be sufficiently low in order to permit the neglection of $(Q_AQ_B)^-$ reoxidation kinetics in the time-scale of measurement (usually 5–10 ms). (3) $Fe(CN)_3$ concentration must not be too high to oxidize Q_{400}, which provides one extra electron acceptor pool on the first flash illumination. Accordingly, we first tried to find $Fe(CN)_3$ concentrations which sufficiently satisfy these requirements for our PS II preparation from *S. vulcanus*.

Fig. 1 shows the absorption changes at 25 °C of our PS II particles at 320 nm, the wavelength where the binary oscillation due to (Q_AQ_B) redox reactions is expected to be maximal [13,21,25]. In the absence of $Fe(CN)_3$ (top traces), the first flash induced a large absorption increase, followed by an at least biphasic decay. The fast relaxation comprises about 25% of the total extent and can be ascribed to formation of Q_B^{2-} in those centers where Q_B^- stayed reduced in darkness. The amplitude of the initial absorption increase caused by the second flash was smaller by 30–40% than that after the first flash, and the initial signal rise was followed by a decay with a half-time of 1–1.5 ms. Although this decay time coincides with those reported for $Z^{ox}S_3 \rightarrow ZS_0$ transition [15,17,22] (Z, the secondary donor of PS II), we ascribe it as due to the electron transfer from Q_A^- to Q_B, substantially retarded by the low temperature (25 °C) effect in this thermophilic cyanobacterium preparation (Tanaka, Y., Satoh, K. and Katoh, S., personal communication). This view is also evident from the observations that the decay component is eliminated by 50 μM $Fe(CN)_3$ (see middle traces of Fig. 1) and that the proportion of the S_3 state after the first flash is negligibly small (Fig. 3). The smaller size of the initial absorbance increase on the second flash implies that in 30–40% of the reaction centers, the Q_A^- formed by the first flash remained reduced during the flash interval (1 s). This contrasts with the situation reported for PS II particles from higher plants, but seems to be common for PS II particles from (thermophilic) cyanobacteria [25]. On the third flash, the initial signal amplitude decreased further, followed by a similar decay kinetics as observed after the second flash. In spite of the similarity in decay time, this component should be ascribed to $Z^{ox}S_3 \rightarrow ZS_0$ transition, since its extent is not affected but pronounced by 50 μM $Fe(CN)_3$ (see middle traces of Fig. 1) and its decay rate coincides well with those reported for $Z^{ox}S_3 \rightarrow ZS_0$ transition [15,17,22]. After the fourth flash, the initial signal amplitude decreased much more, followed by the same decay kinetics. In this case, the decay may comprise both components, Q_A^- to Q_B electron

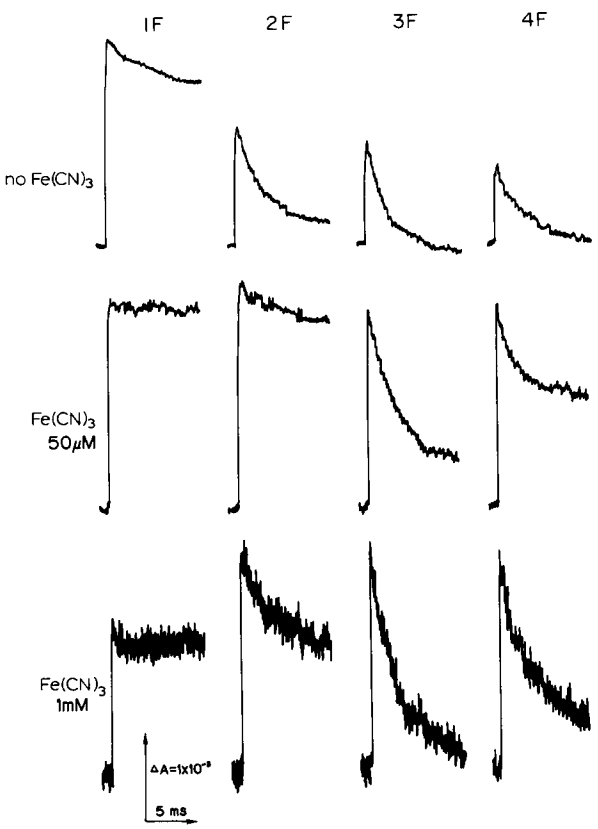

Fig. 1. Flash-induced absorption changes at 320 nm in dark-adapted O_2-evolving PS II particles of *S. vulcanus* in the absence and presence of $Fe(CN)_3$. Flashes were given at 1 Hz and two measurements were averaged. Top, no $Fe(CN)_3$; middle, 50 μM $Fe(CN)_3$; bottom, 1 mM $Fe(CN)_3$.

transfer and $Z^{ox}S_3 \rightarrow ZS_0$ transition. After the fifth or more flashes, the signal further decreased in its initial amplitude, to be practically non-detectable (data not shown). This is due to gradual filling up of Q_A, which we have separately confirmed by means of thermoluminescence measurement (unpublished data). Probably, the acceptor pool size is much limited in cyanobacterial PS II preparations [26,27].

In the presence of 50 μM $Fe(CN)_3$ (middle traces) the flash-induced absorption changes remained almost constant in their initial amplitudes, but depended strongly in their decay kinetics on the flash number within the train: there was practically no decay with half-time of 1–1.5 ms after the first and second flash, but a marked decay was observed after the third and fourth flashes. That there was practically no decay after the first flash indicates the absence of stable Q_B^- in the initial dark-adapted condition. The similarity in the initial signal amplitude regardless of the flash number indicates the absence of photoaccumulation of Q_A^-, and in turn the almost complete oxidation by $Fe(CN)_3$, in the flash intervals of 1 s, of $(Q_AQ_B)^-$ generated by a previous flash. Importantly, the extent of the decay after the second flash in the presence of 50 μM $Fe(CN)_3$ was very slight as compared with that in the absence of $Fe(CN)_3$. This indicates that the binary oscillations due to $(Q_AQ_B)^-$ were mostly overcome by the presence of 50 μM $Fe(CN)_3$. In this context, the redox status of Q_{400}, which has been identified as the endogenous high-spin Fe^{2+} located between Q_A and Q_B [29–31], must be taken into account since it is appreciated that the decay due to the binary oscillation may manifest after the third flash, if Q_{400} has been oxidized in the initial dark-adapted condition. However, this possibility can be ruled out by the observations that the initial signal amplitude after the first flash in the presence of 50 μM $Fe(CN)_3$ was the same as that in the absence of $Fe(CN)_3$ (Fig. 1(1F), top trace), but was twice as large as that in the presence of 1 mM $Fe(CN)_3$ (Fig. 1(1F), bottom trace); $Fe(CN)_3$ at 1 mM was shown to oxidize in darkness the Q_{400} in our preparation (see also Fig. 2).

Now that the binary oscillations due to acceptor side are eliminated, we can interpreted the traces in the middle row of Fig. 1 as follows: the initial signal rise in the presence of $Fe(CN)_3$ comprises at least two components; one is the contribution by the acceptor side, Q_A^-, and the other is that by the donor side reactions (S-state transitions and redox reaction of Z, particularly after the third flash). At this measuring wavelength (320 nm), approx. 75% of the initial signal amplitude is calculated to be the contribution by the former component, according to the method described in Refs. 16, 17, and 28. Under flash trains, the former component will repeatingly exhibit contribution of the same size, since all the confusing effects due to the acceptor side (binary oscillation, photoaccumulation of Q_A^- and dark oxidation of Q_{400}) have been overcome by 50 μM $Fe(CN)_3$. In contrast, the latter component does not decay in the flash intervals of 1 s but accumulates during the first two flashes, and then suddenly will undergo a 1–1.5 ms decay accompanying the $Z^{ox}S_3 \rightarrow ZS_0$ reaction on excitation of the S_3 state by the third flash. This is the scenario of the absorption changes in ultraviolet region proposed by many earlier investigators [15,17,22,32], and our data in the presence of 50 μM $Fe(CN)_3$ can be well accounted for by this scenario.

At a higher concentration of $Fe(CN)_3$ (1 mM), the initial signal amplitude after the first flash was lower than that after the following flashes (bottom traces). The small size that is specific for the absorption change after the first flash has been reported for trypsinized PS II particles [15], and this can be attributed to oxidation of Q_{400} [29,30], an Fe^{2+} center located between Q_A and Q_B [31]. Notably, the amplitudes after the second and subsequent flashes were almost the same as those in the presence of 50 μM $Fe(CN)_3$, and their absorbance decays were markedly faster than those at 50 μM $Fe(CN)_3$. This is probably due to reoxidation of $(Q_AQ_B)^-$ accelerated by the high concentration of $Fe(CN)_3$ during the time-scale of absorption measurement.

The data of Fig. 1 suggest that the $Fe(CN)_3$ concentration which minimizes the binary-type absorption changes is around 50 μM. However, the wavelength of the measuring beam used for Fig. 1 experiments (320 nm) is not always the best wavelength for detection of the absorption changes due to S-state transitions, since Z is reported to have an appreciable extinction coefficient at 320

nm in its oxidized form [14,21,23,25]. Thus, we performed similar experiments at 350 nm where the redox reaction of Z has been reported to show no or minimal absorption change [14,21,23,25].

Fig. 2 compares the $Fe(CN)_3$ titration experiments at 320 and 350 nm, in which the initial signal amplitudes after the first four flashes are plotted against $Fe(CN)_3$ concentration. As shown by panel A, the signal amplitude at 320 nm after the first flash was constant up to 50 μM and decreased at higher concentrations, indicative of oxidation of Q_{400} at high concentration of $Fe(CN)_3$ [15]. The signal amplitudes after the second, third and fourth flashes increased with increasing $Fe(CN)_3$ concentration and reached approximately the same saturation level above 50–100 μM. These profiles indicate that efficient oxidation of $(Q_AQ_B)^-$ in the flash interval of 1 s is achieved at 50 μM $Fe(CN)_3$.

Our titration data of Q_{400} by $Fe(CN)_3$ are in good agreement with the titration curve reported by Petrouleas and Diner [31], who assumed Q_{400} as Fe^{2+}, between Q_A and Q_B, having no extinction at this wavelength. However, both the result by us and by Petrouleas and Diner cannot be explained by the difference spectrum reported by Dennenberg and Jursinic [28], who observed a $(Q_{400}\text{-}Q^+_{400})$ difference spectrum very similar to the difference spectrum of (semiquinone-quinone): If this is the case, dark Q_{400} oxidation will not reduce the initial signal amplitude at 320 nm. At present, we can provide no relevant reason for this discrepancy but to point out a difference in the experimental condition: a short 5–7 ns laser was used as the actinic light in this study, while a longer 3-μs flash was used in [28].

Fig. 2(B) shows the results of similar titration experiments at 350 nm. The signal amplitude after the first flash was constant up to 50 μM $Fe(CN)_3$, but started to decrease appreciably above 100 μM, due to Q_{400} oxidation. The signal amplitudes after the second, third and fourth flashes increased gradually with increasing $Fe(CN)_3$ concentration and reached their respective saturating levels above 50 μM. The same signal amplitude after the first and second flashes at 50 μM $Fe(CN)_3$ suggests that the extinction coefficients of $S_1 \rightarrow S_2$ and $S_2 \rightarrow S_3$ transitions are practically the same at 350 nm, because the absorption change due to $(Q_AQ_B)^-$ does not depend on flash number at 50 μM $Fe(CN)_3$, and Z^{ox} is assumed to show no absorption change at 350 nm. This result agrees with the previous reports by Dekker et al. [22] and Saygin and Witt [20].

The initial signal amplitude after the third flash was appreciably lower than that after the first and second flashes at 350 nm, in contrast to the markedly less pronounced differences at 320 nm. This phenomenon can be explained by differences in $\Delta\epsilon(Z^{ox}/Z)$ at 320 and 350 nm. At 350 nm

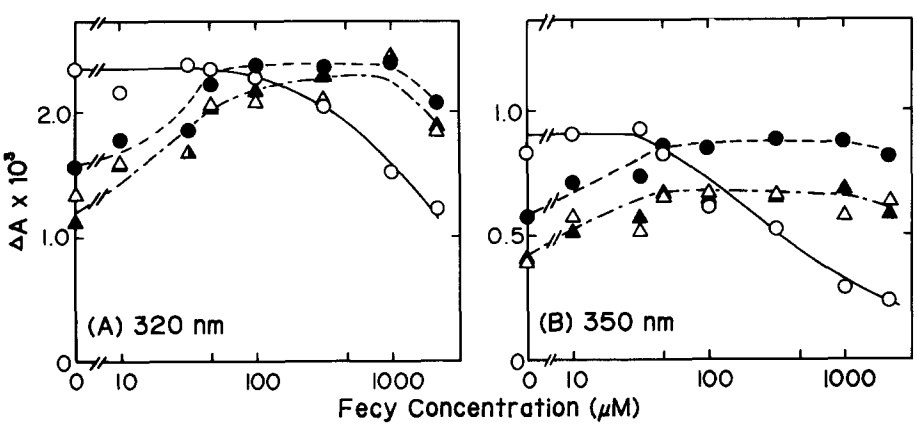

Fig. 2. Effect of $Fe(CN)_3$ concentration on the initial amplitude of absorbance changes. Samples were illuminated with the first to fourth flashes and the initial signal amplitudes were measured at 320 (A) and 350 nm (B) with the same sweep-time as in Fig. 1. Signal accumulations were 2- and 4-times for (A) and (B), respectively. ○, First flash; ●, second flash; △, third flash; ▲, fourth flash.

$\Delta\epsilon(Z^{ox}/Z)$ is negligibly small, and therefore the contribution from reactions at the donor side are almost entirely due to $S_i \rightarrow S_{i+1}$ transitions. In the third flash the majority of the water-oxidizing enzyme systems undergoes the $S_3 \rightarrow (S_4) \rightarrow S_0$ reaction, giving rise to an absorption decrease, and therefore a smaller initial amplitude is expected. On the other hand, at 320 nm $\Delta\epsilon(Z^{ox}/Z)$ was found to be significant [14,21,23,25], so that Z oxidation markedly contributes to the initial increase of absorption.

A different pattern is expected for the absorption changes at 350 nm induced by the fourth flash. In this case the extent of the absorption increase should be larger than after the third flash, because of the $S_0 \rightarrow S_1$ transition in an appreciable fraction of water-oxidizing enzyme systems. This was found not to be the case. This effect can be explained by the assumption that $\Delta\epsilon(S_0 \rightarrow S_1)$ is markedly smaller than $\Delta\epsilon(S_1 \rightarrow S_2)$ and $\Delta\epsilon(S_2 \rightarrow S_3)$ at 350 nm [16,20]. However, the present data do not permit us to quantify this difference.

Apart from these detailed interpretation of the signal amplitude at the two wavelengths, the data in Fig. 2 clearly indicate that the absorption changes due to S-state transitions can be measured at 350 nm without or with minimized distortion due to the acceptor side effects, if we include 50 μM $Fe(CN)_3$ in the reaction medium. In order to confirm this further, we measured as a function of flash number the extent of relaxation kinetics with half-lifetimes of the order of 1 ms.

As shown in Fig. 3(A), the extent of the 1–1.5 ms decay component showed a period four oscillation having maxima at the third and seventh flashes. This oscillation pattern agreed appreciably with that of the O_2 yield in a flash train shown in Fig. 3(B). The oscillation can be satisfactorily described by the Kok model, with $S_1 : S_0 = 75 : 25$, 6% misses and 8% double hits (the relatively high double hits despite the 5–7 ns flash is due to strong measuring light [32]). Furthermore, the oscillation pattern of the absorbance changes showed a two-digit phase shift on addition of a low concentration (10–30 μM) of NH_2OH (data not shown). These data clearly indicate that the signal decay measured under the present conditions unambiguously reflects the absorbance change due to $S_3 \rightarrow S_0$ transition. The oscillation

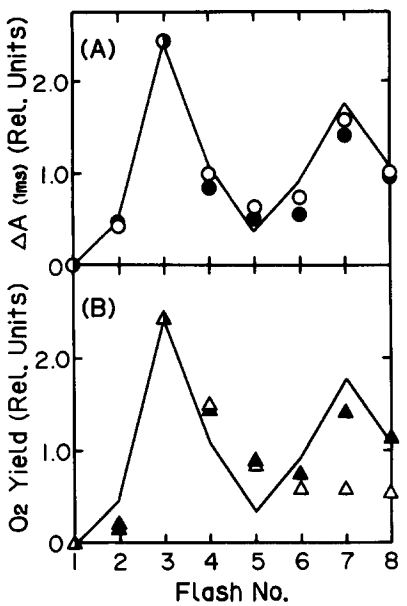

Fig. 3. Flash number-dependent oscillation of the amplitude of absorbance decay with approx. 1 ms half-time (A) and flash O_2 yield (B). $Fe(CN)_3$ concentration was 50 μM and the other experimental conditions for absorption measurements are the same as in Figs. 1 and 2. The absorbance decay at 320 (●) and 350 nm (○) in 5 ms after the flash were plotted. Flash O_2 yield was measured at 25 °C in the presence (▲) and absence (△) of 500 μM $Fe(CN)_3$. The solid line indicates a simulation of $S_3 \rightarrow S_0$ transition, assuming 6% misses and 8% double hits with $S_1 : S_0 = 75 : 25$ in the initial dark-adapted condition (apparent ratio, see Ref. 42).

pattern of the O_2 yield per flash was slightly more damped than that of the extent of the 1 ms relaxation kinetics. This is probably because the $Fe(CN)_3$ concentration was not high enough to oxidize effectively the acceptor side during the dark time between the flashes in thick PS II particles in Joliot electrode experiments. This has been separately confirmed by means of thermoluminescence measurements (unpublished data).

Temperature dependence of the S-state transitions in S. vulcanus PS II particles

The PS II particles from *S. vulcanus* retain the thermophilic characteristics after their isolation from thylakoids and exhibit maximal O_2 evolution at 50–55 °C, and the activity declines with lowering the ambient temperature [5]. As discussed in the previous section, it is now possible to measure

the flash number-dependent absorption changes due to the S-state transitions in our PS II particles, with minimal contribution of Z^{ox} absorption (at 350 nm in the presence of 50 μM $Fe(CN)_3$). Although the target signals are superimposed by a constant level of the initial absorption increase due to Q_A^- formation, the relaxation kinetics of Q_A^- is sufficiently slow to be negligible in the time scale of our measurements in the presence of 50 μM $Fe(CN)_3$ (Fig. 1).

Fig. 4 depicts the absorption changes at 350 nm observed at three different temperatures after the first, second and third flash illumination of dark-adapted PS II particles in the presence of 50 μM $Fe(CN)_3$. On the first flash illumination at 50 °C, the optimal temperature for O_2 evolution by our PS II particles [5], an instantaneous absorption increase took place, which was followed by a slower rise accomplished within 1 ms. The rising component which cannot be resolved due to the limited time resolution (1–2 μs) of our equipment is ascribed to reduction of Q_A and the slowly rising component is mainly due to $S_1 \rightarrow S_2$ transition. From this profile, the half-rise time for $S_1 \rightarrow S_2$ transition was determined to be 60 μs. On lowering the ambient temperature, the kinetics of the slowly rising phase was slowed down, showing half-rise times of 70 and 106 μs at 25 and 1 °C, respectively. Notably, the amplitude of the instantaneous rise was kept almost constant either after the first or second flash independent of ambient temperature. The second flash induces the $S_2 \rightarrow S_3$ transition in most of the water-oxidizing enzyme systems. In a first-order approximation contributions due to $S_1 \rightarrow S_2$ and $S_3 \rightarrow S_0$ transitions can be neglected. Thus, we could similarly determine the half-times of the $S_2 \rightarrow S_3$ transition at 50, 25 and 1 °C as 60, 120–150 and 300 μs, respectively, from the rise kinetics of the absorption changes induced by the second flash.

The traces on the right column of Fig. 4 show the absorbance changes after the third flash. Note that the sweep-time is 5-times slower than that after first and second flashes. The initial signal amplitude appeared slightly but reproducibly higher than those after the first and second flashes. At 50 °C, the fast initial absorbance rise was immediately followed by a 1–1.5 ms decay, but at lower ambient temperatures the decay was preceded by a slight lag period, particularly at lower temperatures. Both the higher initial signal amplitude and the lag period are probably due to the contribution by the absorbance increase due to $S_2 \rightarrow S_3$ (and $S_1 \rightarrow S_2$) transition in a minor population (approx. 25%) of the water oxidation systems. In fact, the profiles measured with 1 ms sweep-time clearly resolved the instantaneous absorbance rise due to Q_A^- formation (with the same

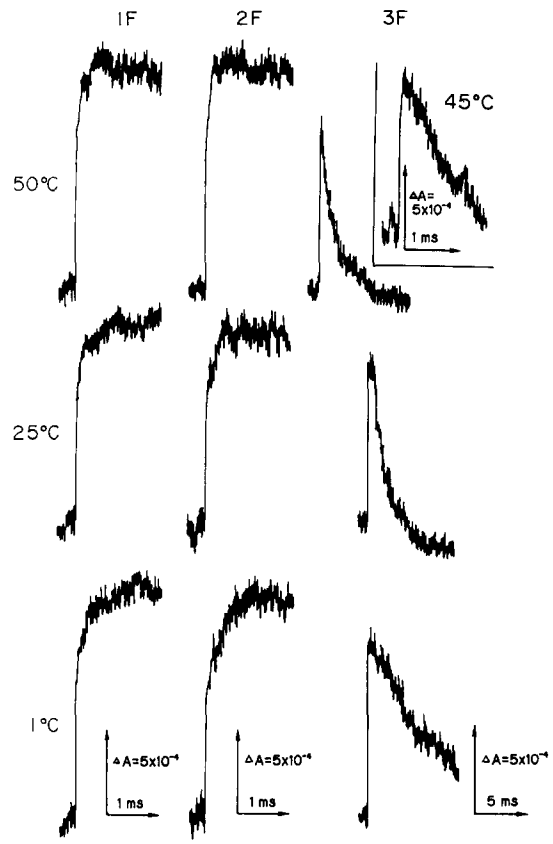

Fig. 4. Flash-induced absorbance changes in dark-adapted PS II particles of *S. vulcanus* at three different temperatures. Samples were illuminated with the first to third flashes in the presence of 50 μM $Fe(CN)_3$, and the absorbance changes were measured at 350 nm. Profiles after the first and second flashes were obtained by averaging 64 signals, and those after the third flash were by four signals. Note that the sweep-time for the third flash measurements was slower (by a factor of 5) than that for the first and second flash measurements. Flash repetition rate was 1 Hz for experiments at 50 and 25 °C, but was reduced to 0.33 Hz for 1 °C experiment. The trace in the margin is the third flash profile at 45 °C measured with a faster (1 ms) sweep-time.

size as observed after first and second flashes), which was followed by a slightly slower absorbance rise due to $S_2 \rightarrow S_3$ (and $S_1 \rightarrow S_2$) transition even at a high temperature of 45 °C (see the trace in the margin of Fig. 4). The presence of a lag period in the third flash profiles is consistent with the previous observations by Dekker et al. [33] and Renger and Weiss [15].

Estimation of the half-times of the 1–1.5 ms decaying component was disturbed by this lag effect. In order to avoid this (and also due to the limited memory size of our equipment), we determined the initial starting level of the decay by extrapolating the decay curve to time zero on a 1 ms sweep-time profile and the finally decayed level of the component on a 5 ms (or slower for experiments at lower temperatures) sweep-time profile, and then, from these two levels, the half-decay times were estimated. Note that the above-mentioned finally decayed level is usually lower than the baseline level, since this component involves the decay of the species accumulated by the previous first and second flashes. It may also be worthwhile to note that the extent of this decay component thus estimated showed maxima at the third and seventh flash, indicative of the absorbance change due to $S_3 \rightarrow S_0$ transition (see Fig. 3). The half-times thus determined were 0.8, 1.3 and 5.5 ms at 50, 25 and 1 °C, respectively. More or less the same values were obtained by another method of half-time estimation, in which we set aside the initial part of the kinetics affected by the lag and estimated the half-time from the normally decaying part of the kinetic profiles. The similarity in half-times obtained by the two different methods is consistent with the view that the absorbance increase due to $S_2 \rightarrow S_3$ transition superimposed on the third flash profile is accomplished at most (at 1 °C) in 1–2 ms (see 2F trace in Fig. 4, bottom) and does not much decay during the measuring time scale, and in turn implies that the 1–1.5 ms decay comprises only one major exponentially decaying component.

The half-times thus determined at three different temperatures are summarized in Table I in comparison with the values at 25 °C reported by other investigators. Our 25 °C data are in appreciable agreement with those reported previously within the fluctuations of this type of measurements. As to the temperature dependence of the half-times for individual S-state transitions, the following characteristics can be pointed out: (1) The $S_2 \rightarrow S_3$ transition shows a stronger temperature dependence than the $S_1 \rightarrow S_2$ transition; the half-time of the former transition increased by 1.2- and 1.5-fold on lowering the ambient temperature from 50 to 25 °C and 25 to 1 °C, respectively, whereas the half-time of the latter transition increased 2.5- and 2.0-fold, respectively, on the same changes in the ambient temperature. (2) The $S_3 \rightarrow S_0$ transition shows also a strong temperature dependence, but its features are different from those of $S_1 \rightarrow S_2$ and $S_2 \rightarrow S_3$ transitions: the half-decay time increased by 1.6-fold on lowering the temperature from 50 to 25 °C, but remarkably by 4.2-fold on lowering from 25 to 1 °C. The dramatic increase in the half-decay time below 25 °C suggests that the $S_3 \rightarrow S_0$ transition involves

TABLE I

HALF TIMES OF S-STATE TRANSITIONS AT THREE DIFFERENT TEMPERATURES IN *S. VULCANUS* IN COMPARISON WITH THOSE REPORTED BY OTHER INVESTIGATORS

Temperature (°C)	S-state transition			Material (Ref.)
	$S_1 \rightarrow S_2$	$S_2 \rightarrow S_3$	$S_3 \rightarrow S_0$	
50	60 μs	60 μs	0.8 ms	*S. vulcanus* [a] (this paper)
25	70 μs	120–150 μs	1.3 ms	
1	106 μs	300 μs	5.5 ms	
25	110 μs	220 μs	1.2 ms	spinach [15]
	70 μs	–	approx. 1 ms	spinach [17]
	110 μs	350 μs	1.3 ms	spinach [28]
	40 μs	80–150 μs	1.2 ms	*Synechococcus* sp. [a] [20]

[a] Thermophilic cyanobacteria.

an anomalous change in activation energy in this temperature range. In order to analyze this anomaly more precisely, we used the conventional Arrhenius plot for S-state transitions.

Fig. 5 shows the reciprocal half-times of individual S-state transitions as a function of $1/T$. The plots for the $S_1 \rightarrow S_2$ and $S_2 \rightarrow S_3$ transitions showed that the data can be described by straight lines between 50 and 1°C without any break or discontinuity, and the activation energies for the two transitions were determined to be 9.6 and 26.8 kJ/mol, respectively. In contrast to these two transitions, the plot for the $S_3 \rightarrow S_0$ transition was composed of two straight lines with a clear break point at around 16°C, and the apparent activation energies above and below the break temperature were 15.5 and 59.4 kJ/mol, respectively. The results obtained in this study reveal remarkable differences for the dynamics of the redox state transitions in the water-oxidizing enzyme system. Two effects are remarkable: (a) the significant difference of the activation parameters for the reactions $Z^{ox}S_1 \rightarrow ZS_2$ and $Z^{ox}S_2 \rightarrow ZS_3$, and (b) the comparatively sharp break point at around

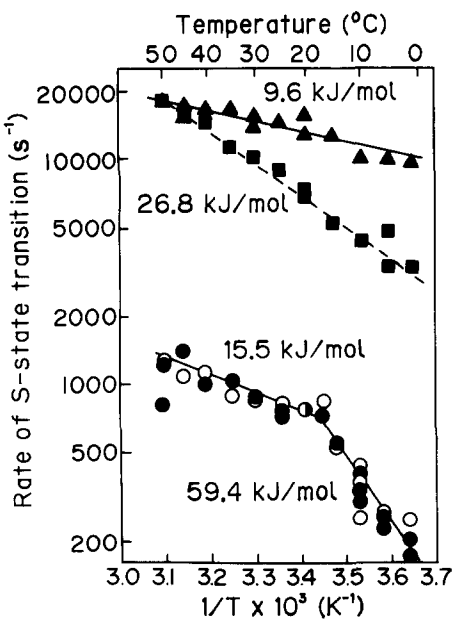

Fig. 5. Arrhenius plots of the rates of S-state transitions. Experimental conditions are the same as in Fig. 4. ▲, $S_1 \rightarrow S_2$: ■, $S_2 \rightarrow S_3$; ●, $S_3 \rightarrow S_0$ transitions determined at 350 nm. ○, $S_3 \rightarrow S_0$ measured at 320 nm.

16°C of the activation process for the reaction sequence $Z^{ox}S_3 + 2H_2O \rightarrow ZS_0(2H) + O_2 + 2H^+$.

From the half-times of S-state transitions shown in Table I, the activation entropies for $S_1 \rightarrow S_2$ and $S_2 \rightarrow S_3$ reactions were calculated, which gave negative values for both reactions. Furthermore, the activation entropy for oxidation of S_1 was markedly more negative than that for S_2 (-140 vs. -85 $J \cdot mol^{-1} \cdot K^{-1}$). This implies that the transition $S_1 \rightarrow S_2$ would require a more pronounced structural ordering than $S_2 \rightarrow S_3$. This would be in line with recent conclusions [34] claiming that the conformation of S_0 and S_1 markedly differs from that of S_2 and S_3. Another difference that would be of mechanistic relevance is the deprotonation step coupled with S_2 oxidation, which is not involved in S_1 oxidation [35–37]. However, as the origin of the protons released in individual redox steps is still not yet clarified [38], we will refrain from any speculation in this direction.

A very interesting finding of this study is the break point in the activation process for $Z^{ox}S_3 + 2H_2O \rightarrow ZS_0(2H) + O_2 + 2H^+$. A comparison of the half-times of Z^{ox} reduction [24] and O_2 release [39] indicates that in spinach thylakoids the electron abstraction from S_3 is the rate-limiting step of the overall reaction at room temperature. If one assumes the same to be true for cyanobacteria, the remarkable break point suggests the existence of two different conformational states of the water-oxidizing enzyme system in the redox state S_3 below and above the critical temperature, T_c. It is very interesting to speculate about the possible formation of a peroxide-like structure in S_3, as discussed previously [40]. In this case, temperature-dependent redox equilibria could exist between manganese and its associated ligands [38,41], permitting the formation of a (0-0) bond in S_3 at the peroxide level above T_c. However, as the break point is very sharp, a phase transition of the whole membrane ensemble might be involved.

Another interesting phenomenon which should be mentioned is that this break temperature coincides with the threshold temperature where the $S_3 \rightarrow S_0$ transition measured by means of thermoluminescence becomes markedly retarded [8]. Interestingly enough, this threshold temperature is markedly lower in spinach thylakoids. Extrapolat-

ing from the present data, the break point in the Arrhenius plot for $S_3 \rightarrow S_0$ could be expected at around 0 °C in spinach thylakoids. By analogy with these, a break of activation energy might be expected at around −40 and −20 °C for $S_1 \rightarrow S_2$ and $S_2 \rightarrow S_3$ transitions, respectively, from the threshold temperatures determined by thermoluminescence measurements [8]. However, we have to keep in mind that these temperatures are far below the freezing point of water, and no ultraviolet absorption transients are available at present at such low temperatures.

Further experiments are required to analyze in full detail the mechanistic implications of the present study about the dynamics of the S_i-state transitions.

Acknowledgements

This work was supported by Deutsche Forschungsgemeinschaft (Sfb 312) and by a grant for Solar Energy Conversion by Means of Photosynthesis at the Institute of Physical and Chemical Research (RIKEN) given by the Science and Technology Agency of Japan. H.K. was a visiting researcher at the Max-Volmer-Institut supported by the Versailles Summit Cooperation Program on Photosynthesis and Photoconversion. The authors are grateful to Dr. M. Völker for his help and encouragement during this study.

References

1 Castenholz, R.W. (1969) Bacteriol. Rev. 33, 476–504
2 Yamaoka, T., Satoh, K. and Katoh, S. (1978) Plant Cell Physiol. 19, 943–954
3 Yamaoka, T., Satoh, K. and Katoh, S. (1978) in Photosynthetic Oxygen Evolution (Metzner, H., ed.), pp. 105–116, Academic Press, London
4 Hirano, M., Satoh, K. and Katoh, S. (1981) Biochim. Biophys. Acta 635, 476–487
5 Koike, H. and Inoue, Y. (1983) in The Oxygen Evolving System of Photosynthesis (Inoue, Y., Crofts, A.R., Govindjee, Murata, N., Renger, G. and Satoh, K., eds.), pp. 257–263, Academic Press, Tokyo
6 Inoue, Y. and Shibata, K. (1978) FEBS Lett. 85, 193–197
7 Demeter, S., Rosza, Zs., Vass, I. and Hideg, E. (1985) Biochim. Biophys. Acta 809, 379–387
8 Koike, H. and Inoue, Y. (1987) in Progress in Photosynthesis Research (Biggins, J., ed.), Vol. I, pp. 645–648, Martinus Nijhoff, Dordrecht
9 Brudvig, G.W., Casey, J.L. and Sauer, K. (1983) Biochim. Biophys. Acta 723, 366–371
10 Rutherford, A.W., Crofts, A.R. and Inoue, Y. (1982) Biochim. Biophys. Acta 682, 457–465
11 Rutherford, A.W., Renger, G., Koike, H. and Inoue, Y. (1984) Biochim. Biophys. Acta 767, 548–556
12 Koike, H. and Inoue, Y. (1985) Biochim. Biophys. Acta 807, 64–73
13 Van Gorkom, H.J. (1974) Biochim. Biophys. Acta 347, 439–442
14 Weiss, W. and Renger, G. (1986) Biochim. Biophys. Acta 850, 173–183
15 Renger, G. and Weiss, W. (1986) Biochim. Biophys. Acta 850, 184–196
16 Pulles, M.J., Van Gorkom, H.J. and Willemsen, J.G. (1976) Biochim. Biophys. Acta 449, 536–540
17 Velthuys, B.R. (1981) in Photosynthesis (Akoyunoglou, G., ed.), Vol. 2, pp. 75–85, Balaban International Scientific Services, Philadelphia
18 Lavergne, J. (1984) FEBS Lett. 173, 9–14
19 Lavergne, J. (1986) Photochem. Photobiol. 43, 311–318
20 Saygin, Ö. and Witt, H.T. (1987) in Progress in Photosynthesis Research (Biggins, J., ed.), Vol. I, pp. 537–540, Martinus Nijhoff, Dordrecht
21 Dekker, J.P., Van Gorkom, H.J., Brok, M. and Ouwehand, L. (1984) Biochim. Biophys. Acta 764, 301–309
22 Dekker, J.P., van Gorkom, H.J., Wensink, J. and Ouwehand, L. (1984) Biochim. Biophys. Acta 767, 1–9
23 Diner, B.A. and DeVitry, C. (1984) in Advances in Photosynthesis Research (Sybesma, C., ed.), Vol. IV, pp. 407–411, Martinus Nijhoff/Dr. W. Junk Publishers, Dordrecht
24 Babcock, G.T., Blankenship, R.E. and Sauer, K. (1976) FEBS Lett. 61, 286–289
25 Schatz, G.H. and Van Gorkom, H.J. (1985) Biochim. Biophys. Acta 810, 283–294
26 Bowes, J.M., Stewart, A.C. and Bendall, D.S. (1983) Biochim. Biophys. Acta 725, 210–219
27 Takahashi, Y. and Katoh, S. (1986) Biochim. Biophys. Acta 848, 183–192
28 Dennenberg, R.J. and Jursinic, P.A. (1985) Biochim. Biophys. Acta 808, 192–200
29 Ikegami, I. and Katoh, S. (1973) Plant Cell Physiol. 14, 829–836
30 Bowes, J.M., Crofts, A.R. and Itoh, S. (1979) Biochim. Biophys. Acta 547, 320–335
31 Petrouleas, V. and Diner, B. (1986) Biochim. Biophys. Acta 849, 264–275
32 Renger, G. and Weiss, W. (1983) Biochim. Biophys. Acta 722, 1–11
33 Dekker, J.P., Plijter, J.J., Ouwehand, L. and Van Gorkom, H.J. (1984) Biochim. Biophys. Acta 767, 176–179
34 Preston, C. and Pace, R.J. (1986) Biophys. J. 49, 25a
35 Förster, V. and Junge, W. (1985) Photochem. Photobiol. 14, 183–190
36 Fowler, C.F. (1977) Biochim. Biophys. Acta 459, 351–363
37 Saphon, S. and Crofts, A.R. (1977) Z. Naturforsch. 32c, 617–626
38 Renger, G. (1987) Photosynthetica 21, in the press
39 Joliot, P., Hoffnung, M. and Chaboud, R. (1966) J. Chim. Phys. 63, 1423–1441
40 Renger, G. (1978) in Photosynthetic Water Oxidation (Metzner, H., ed.), pp. 229–248, Academic Press, London
41 Renger, G., Hanssum, B. and Weiss, W. (1987) in Progress in Photosynthesis Research (Biggins, J., ed.), Vol. I, pp. 541–544, Martinus Nijhoff, Dordrecht
42 Vermaas, W., Renger, G. and Dohnt, G. (1984) Biochim. Biophys. Acta 764, 194–202